

# DEVELOPMENT OF RADIATION PROCESSED NANO-COMPOSITE BLENDS AND NANO-COATINGS FOR INDUSTRIAL APPLICATIONS

K.A. Dubey, Virendra Kumar, Yatender Bhardwaj, Chandrasekhar Chaudhari, K.S.S. Sarma, Sheikh Abdul Khader, Satyanarayan Acharya

Bhabha Atomic Research Centre, Trombay, Mumbai- 400 085, India.

## Abstract

Radiation processing of nanoparticle-filled polymer blends and coatings is expected to synergize the benefits of radiation processing and the flexibility of achieving various property combinations. High energy radiation can be utilized in a variety of ways to modify these systems. It can be used to crosslink the matrix, to compatibilize the blend components, to synthesize graft copolymer based compatibilizers, to improve interfacial bonding between the nanofiller/polymers or to freeze the morphology. Properties like flame retardancy, permeability, abrasion resistance, biocompatibility and antibacterial activity can also be significantly affected by this composite approach. Due to the variety and quality of the product it promises, radiation processing of these mixed systems has been our core interest in the last few years. In the report, some of results on the radiation processing of SBR/EPDM blends and SBR/EPDM/MWNT nanocomposites are presented.

## 1. Introduction

The rubber industry has utilized sulfur and accelerator system as a primary tool for vulcanization for years. High-energy ionizing radiation has recently received a great deal of attention, primarily because of its ability to produce cross-linked networks with a wide range of polymers [1-5]. The radiation-vulcanized products offers lower compression set and superior heat aging characteristics than those vulcanized with conventional means. Added advantages of low operation cost, additive free technique and room temperature operations make radiation processing an attractive tool for the development of medical grade and high performance rubbers.

Blending of unsaturated rubbers with saturated rubbers can provide a solution for the inherent structural drawbacks of the unsaturated matrices viz. poor heat and ozone resistance [6-9]. In this regard, radiation processed blends of Styrene-Butadiene Rubber (SBR) and Ethylene-Propylene Diene Monomer (EPDM) rubber envisaged a special interest because incorporation of a suitable amount of EPDM in SBR is expected to impart significant heat and ozone resistance in the SBR matrix while weak adhesion property and poor tear strength of EPDM are expected to be improved substantially with the incorporation of SBR in the EPDM matrix. Furthermore, as radiation crosslinking improves the ozone resistance of SBR matrix, radiation vulcanized SBR/EPDM blends are also expected to offer good weatherability characteristics [10-12].

The properties of SBR/EPDM blends can be further improved by reinforcing SBR/EPDM blends with nanofillers such as Multiple Wall Carbon Nanotube (MWNT). These nanoparticulate filler based SBR/EPDM nanocomposites are expected to transcend conventional filler-elastomer interface limitations and offer high quality products, as even small quantity of these fillers is expected to render superior physical, thermal and mechanical properties than their conventional analogs[13-14].

## 2. Materials & methods

Styrene-Butadiene Rubber (SBR) and Ethylene-Propylene Diene Monomer rubber (EPDM) were supplied by M/s Polystar chemicals, Mumbai. Specifications of the polymers used in the study are mentioned in table 1. All solvents and reagents used in the study were from Aldrich chemicals USA and are of AnalR grade. Industrial grade multiple walled carbon nanotube (Nanocyl™ NC 7000) was procured from Nanocyl Belgium and used in the study without purification.

TABLE 1. SPECIFICATIONS OF POLYMERS USED IN THE STUDY

Name	Specifications
SBR	Styrene content 25 %; Mooney viscosity: ~52 (100 °C); Specific gravity: 0.945
EPDM	Ethylene content 55%; Specific gravity: 0.87; Mooney viscosity ML~+4 of 60 (120°C)

### 2.1. Sample preparation

Blends of SBR and EPDM in different composition were prepared by mixing both the rubbers on a two-roll laboratory mill. A series of nanocomposites of SBR/EPDM 50:50 blend containing different amounts of MWNT was prepared by initially mixing the two components in Brabender plasticodar. The homogeneous mix was cut into small pieces and compressed into sheets of size 12x12 cm<sup>2</sup> of different thicknesses in range 1-4 mm using compression-molding machine at 150 kg/cm<sup>2</sup> pressure for 2 minutes at 130°C. Nanocomposite compositions and sample designations have been represented in Table 2.

TABLE 2. SAMPLE DESIGNATIONS OF SBR/EPDM BLENDS AND NANOCOMPOSITES

Blends			SBR/EPDM 50:50 blends with MWNT		
SBR (%)	EPDM (%)	Designation	Blend	MWNT (%)	Designation
100	00	SE <sub>00</sub>	SE <sub>50</sub>	00	SE <sub>NT00</sub>
75	25	SE <sub>25</sub>	SE <sub>50</sub>	0.5	SE <sub>NT05</sub>
50	50	SE <sub>50</sub>	SE <sub>50</sub>	1.0	SE <sub>NT1</sub>
25	75	SE <sub>75</sub>	SE <sub>50</sub>	3.0	SE <sub>NT3</sub>
00	100	SE <sub>100</sub>	SE <sub>50</sub>	5.0	SE <sub>NT5</sub>

### 2.2. Irradiation

Irradiation of SBR/EPDM blends and all nanocomposites was carried out under aerated condition using a gamma chamber 5000 (GC-5000) having Co-60 gamma source supplied by M/s BRIT India. The dose rate of gamma chamber was ascertained by using Fricke dosimetry prior to irradiation of samples.

### 3. Result and discussion

#### 3.1. Effect of radiation on SBR/EPDM blends

Figure 1 shows the change in the gel content of SBR-EPDM blends on irradiation. Un-irradiated samples were found to be easily soluble in hot xylene, however blends irradiated to a dose  $>20$  kGy were insoluble due to the formation of a three-dimensional network. Sol-gel studies revealed higher sensitivity of EPDM to irradiation, as for a dose of 40 kGy, gel fractions of 94% and 30% were found for pure EPDM and SBR respectively. It was expected that for a particular radiation dose, the gel-content of the blends would lie in between the pure SBR and pure EPDM depending on their composition however, it was interesting to note that the gel content value of  $S_{25}E_{75}$  was very close to pure EPDM whereas  $S_{75}E_{25}$  and  $S_{50}E_{50}$  showed value of gel contents closer to pure SBR in the dose range studied.

Another obvious effect brought about by irradiation on the blends due to their crosslinking/degradation is on their tensile strength. Figure 2 illustrates the tensile strength of the blends as a function of radiation dose. Tensile strength of pure EPDM, pure SBR and their blends were found to increase continuously in the dose range of study. Furthermore, the observed trend for the intermediate blend compositions is on the expected lines i.e. the tensile strength of the blends increases with increase in EPDM content and absorbed dose.

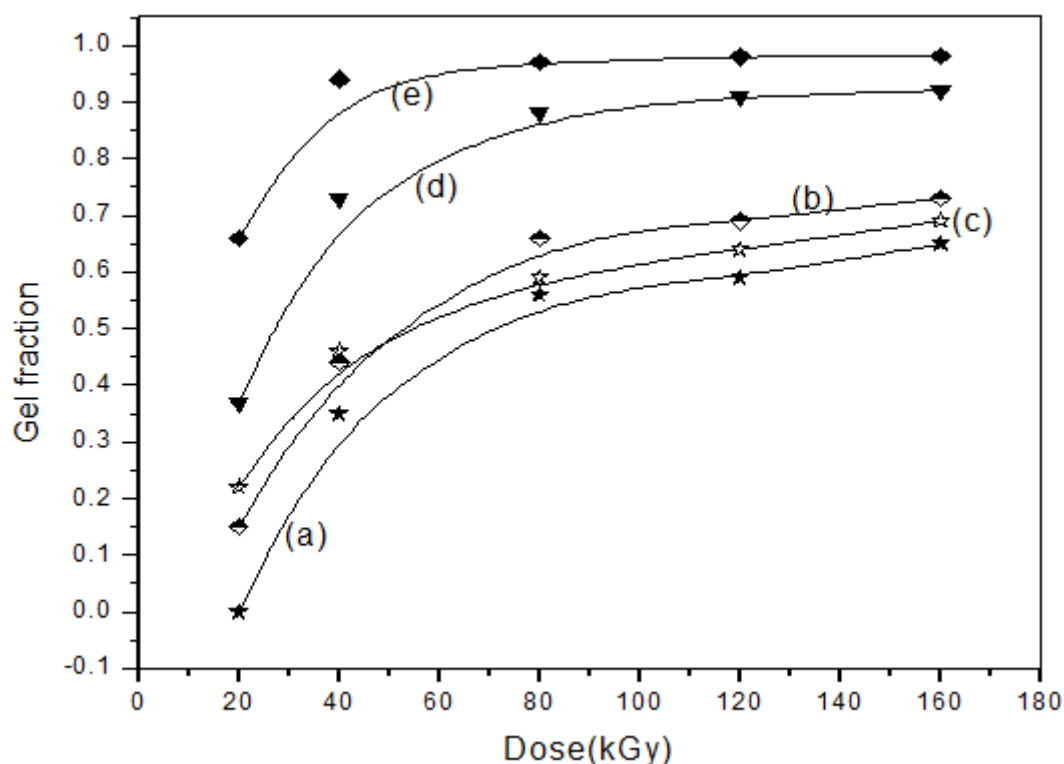


Fig. 1. Change in gel fraction of blends on irradiation at a dose rate of 5 kGyh<sup>-1</sup> for different compositions of SBR/EPDM blends (a) EPDM 0% (b) EPDM 25% (c) EPDM 50% (d) EPDM 75% (e) EPDM 100%.

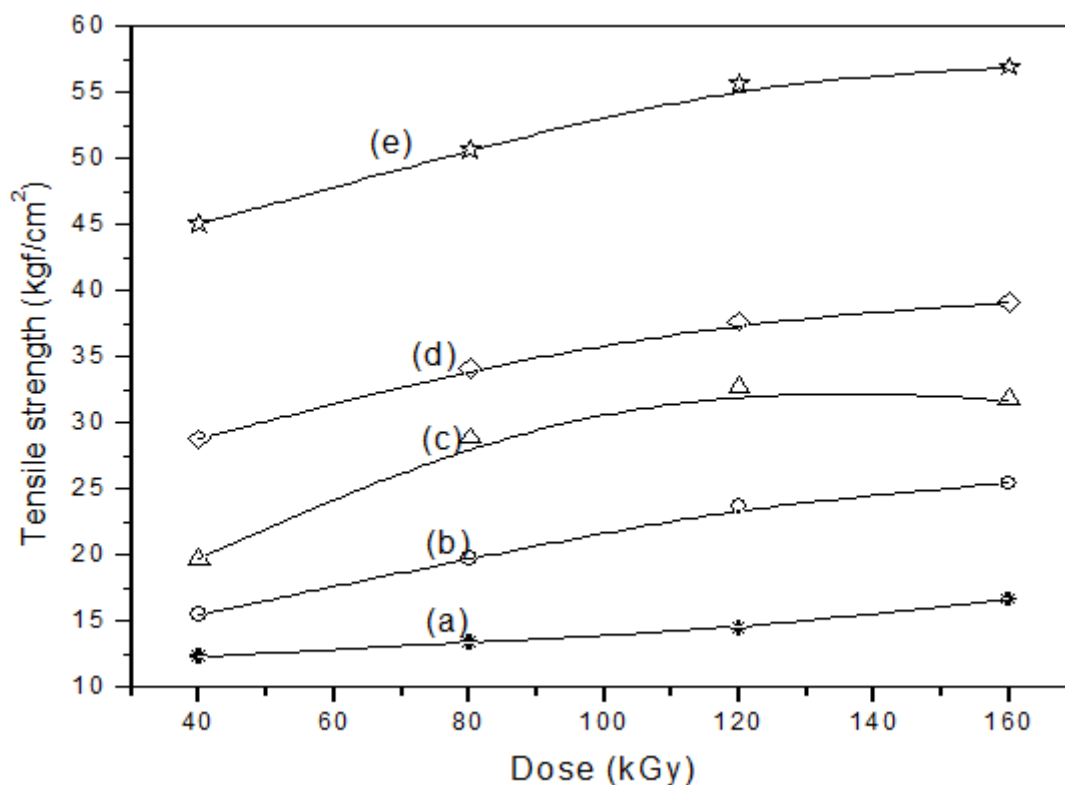
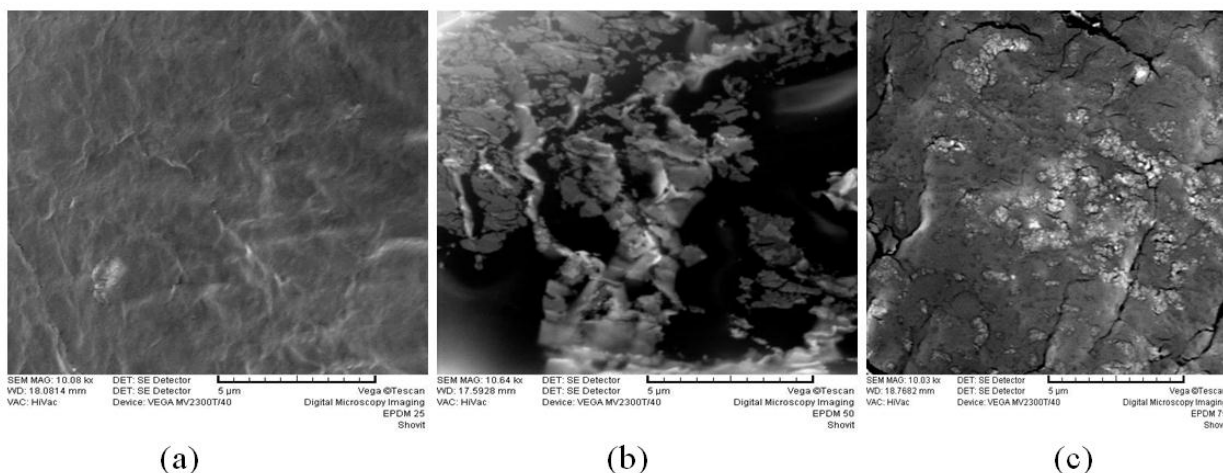


Fig. 2. Change in tensile strength of blends on irradiation at a dose rate of 5 kGyh<sup>-1</sup> for different compositions of SBR/EPDM blends (a) EPDM 0 % (b) EPDM 25 % (c) EPDM 50 % (d) EPDM 75 % (e) EPDM.

### 3.2. Morphology of blends

The scanning electron micrographs of fractured and Os O<sub>4</sub> treated surfaces have been shown in figure 3. For the compositions, S<sub>25</sub>E<sub>75</sub> and S<sub>50</sub>E<sub>50</sub> phase separation can be clearly seen, whereas for the S<sub>75</sub>E<sub>25</sub> it is not that conspicuous. At higher EPDM fractions, the SBR matrix was found to be embedded (disperse phase) in the continuous EPDM phase, whereas, at lower EPDM weight fractions co-continuous morphology of SBR and EPDM were observed. These results resembles to our observations in an earlier investigation on the segmental interactions of EPDM and SBR in the presence of solvent, where, by using solvent permeation techniques, the co-continuous phase of EPDM was established in all the composition range. SEM of the blends also indicated the higher rigidity of EPDM phase in comparison to SBR phase.



*Fig. 3. Scanning electron micrographs of SBR/EPDM blends (a) EPDM 25 %(b) EPDM 50 %(c) EPDM 75 %.*

### **3.3. Effect of the addition of mwnts on the physico-mechanical and radiation vulcanization behaviour of sbr/epdm blends**

Figure 4 shows the change in the gel content of SBR/EPDM/MWNT nanocomposites on irradiation. Un-irradiated samples were found to be easily soluble in hot xylene, however nanocomposites irradiated to a dose >30 kGy were partly insoluble due to the formation of a three-dimensional network. The manifold increase in the mechanical properties of the parent matrices on addition of nanofillers has been attributed to the inherent defect free morphology of the nanofillers. Radiation processing of these nanocomposites may further affect the mechanical properties due to crosslinking/degradation of the polymer matrix. Figure 5 illustrates the tensile strength of the nanocomposites as a function of radiation dose. Tensile strengths of the pure SBR/EPDM (50:50) blend and its nanocomposites were found to increase with dose up to 200 kGy and remain constant thereafter. The trend observed for the intermediate compositions is on the expected lines i.e. the tensile strength of the nanocomposites increased with the increase in MWNT content and with the increase in absorbed dose.

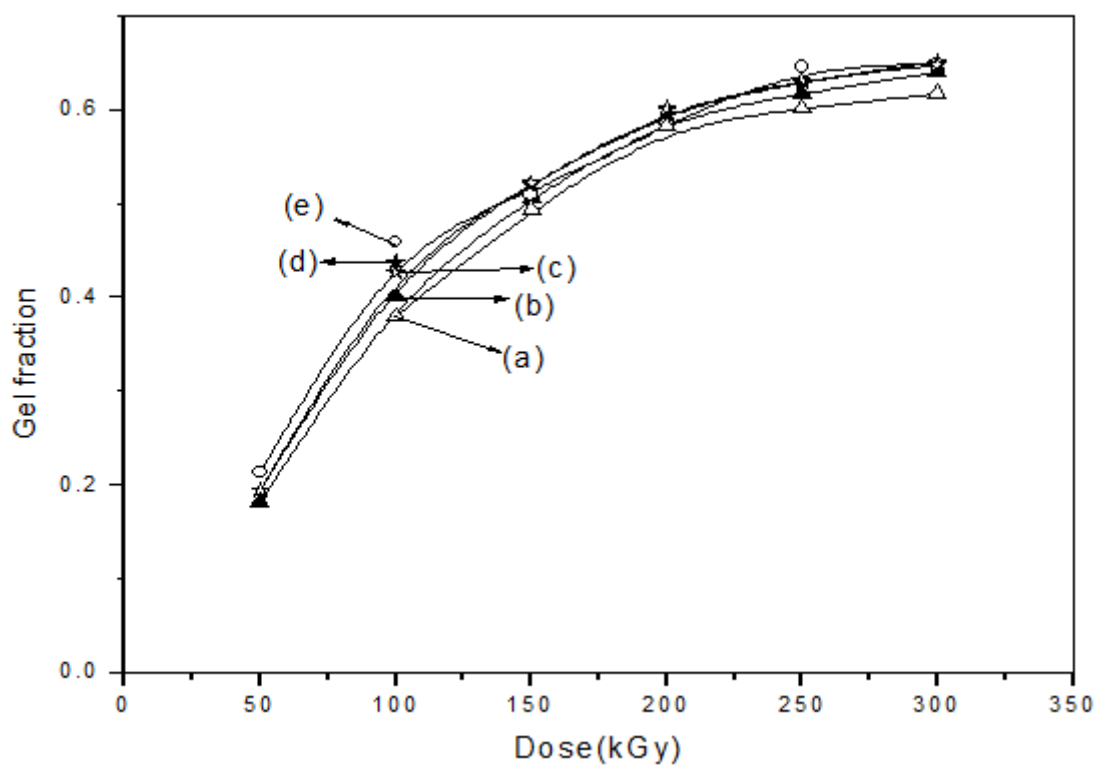


Fig. 4. Gel fraction of nanocomposites on irradiation at a dose rate of  $3.5 \text{ kGyh}^{-1}$  (a)  $SE_{NT00}$  (b)  $SE_{NT05}$  (c)  $SE_{NT1}$  (d)  $SE_{NT3}$  (e)  $SE_{NT5}$

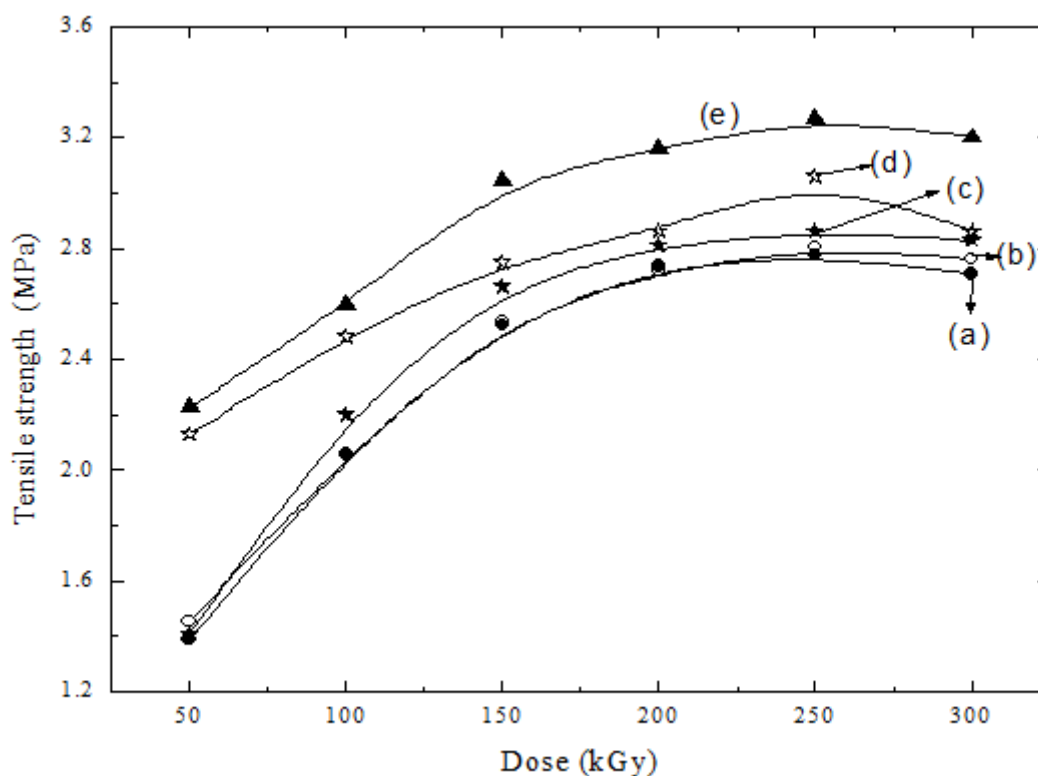


Fig. 5. Tensile strength of nanocomposites on irradiation at a dose rate of  $3.5 \text{ kGy h}^{-1}$  (a)  $SE_{NT00}$  (b)  $SE_{NT05}$  (c)  $SE_{NT1}$  (d)  $SE_{NT3}$  (e)  $SE_{NT5}$

Figure 6 shows the relationship between elongation at break and radiation dose for different samples. The elongation at break decreased with dose for all nanocomposites due to more crosslinked structures produced in the sample matrix, which prevents the structural organization during drawing and brings about a decrease in internal chain mobility and elongation. The rapid decrease of elongation at break with the increasing MWNT loadings, which is observed in many composite systems, is believed to be caused by the premature failure starting at the MWNT aggregates. This reduction in the elongation at break with the addition of MWNT is not unusual for polymers and indicates that interfacial interactions between the elastomer and MWNTs were not sufficient to induce any positive effect on bulk elongation properties. Young modulus of the composites was found to increase with the increase in MWNT content and radiation dose (Figure 7). A significant increase in the Young's modulus was observed when the MWNT content was increased from 1 to 3%. This behavior can be attributed to the structural changes of the composites with the increasing nanotube content, as it has reported that at higher content a continuous MWNT network is formed throughout the matrix, which produces strong mechanical interlocking among nanotubes and promotes the reinforcement.

To understand the nanocomposites' mechanical characteristics, it is essential to compare the experimental results with standard micro-mechanical models developed for such systems. In this study, additive law, Guth model and Halpin-Tsai (HT) equations are used to predict the bulk properties of the carbon nanotube composites[17]. The MWNT diameter, length, and Young's modulus of 20 nm, 50  $\mu\text{m}$  and 400 GPa were used in the calculations. The additive

rule and Guth model were found to be inadequate in expressing the modulus behavior of SBR/EPDM/MWNT nanocomposites as the values calculated were much higher than the experimental and HK values. Though HK results shows slightly lower values than the additive rule, the values were still significantly higher than the experimental results. The deviation of experimental results from the above mentioned models indicates that assumptions, such as homogeneous distribution and efficient transfer of tensile load to the MWNTs, made to derive these equations do not hold good for these nanocomposites. Thus, these models were modified by applying boundary conditions for the elastomer systems and by varying apparent aspect ratio of MWNTs in the elastomer matrix. Figure 7 represents the fitting of Guth and Halpin-Tsai model to modulus variation with volume fraction of MWNT in the dose range studied. While the fitting using Guth model deviates from the experimental results at higher filler loadings, the Halpin-Tsai model shows good agreement within the data obtained. It was interesting to observe that though the aspect ratio estimated using both the models was almost same but it was much less than the actual aspect ratio of MWNT. This finding clearly indicates the presence of agglomerates in the matrix. It has been reported that  $dE_c/dV_f$  can be a good measure of reinforcing efficiency of MWNTs, as it takes into account both magnitude of the modulus increase and the amount of MWNTs required to achieve it [18-19]. Therefore the magnitude of  $dE_c/dV_f$  was estimated for nanocomposites. The increase in magnitude of  $dE_c/dV_f$  (measure of reinforcement) with radiation indicates that there is improvement in load transfer effect on irradiation and an interface link between MWNTs and elastomer matrix is established after radiation treatment. These results support our justification that higher crosslinking yield of nanocomposites containing higher fractions of MWNTs is due to physical crosslinking assisted free volume reduction in the nanocomposite matrix.



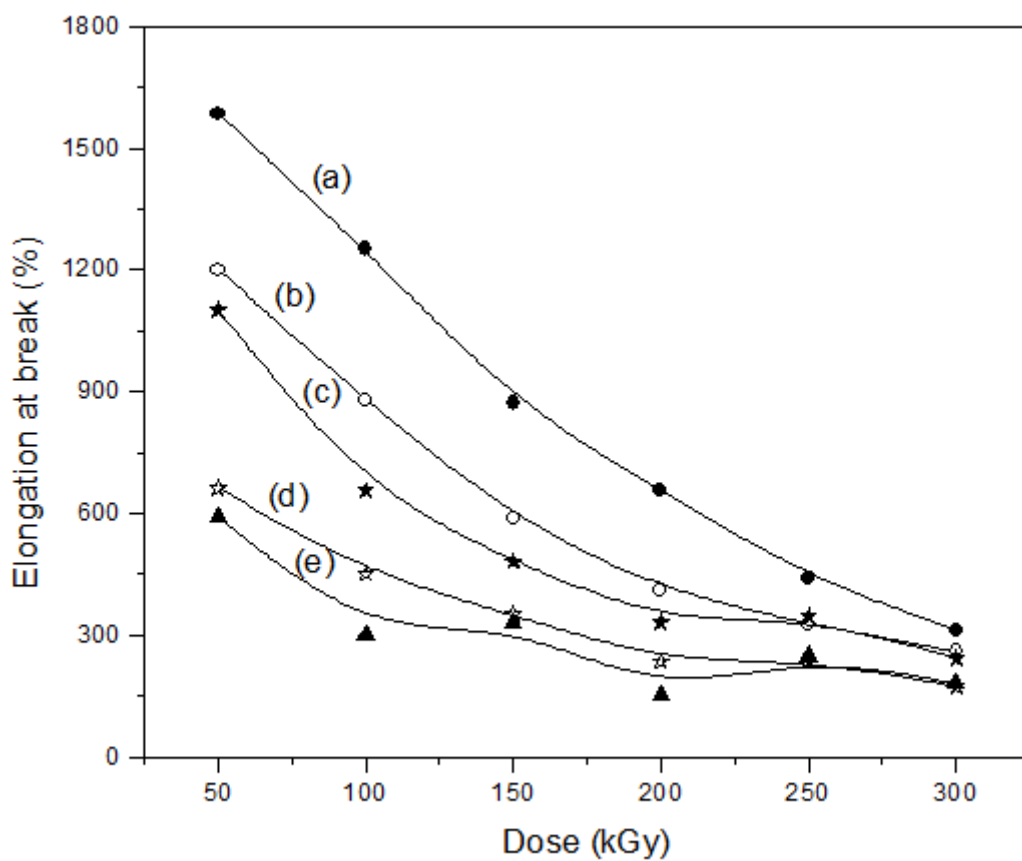


Fig. 6. Elongation at break of nanocomposites on irradiation at a dose rate of  $3.5 \text{ kGyh}^{-1}$  (a)  $SE_{NT00}$  (b)  $SE_{NT05}$  (c)  $SE_{NT1}$  (d)  $SE_{NT3}$  (e)  $SE_{NT5}$

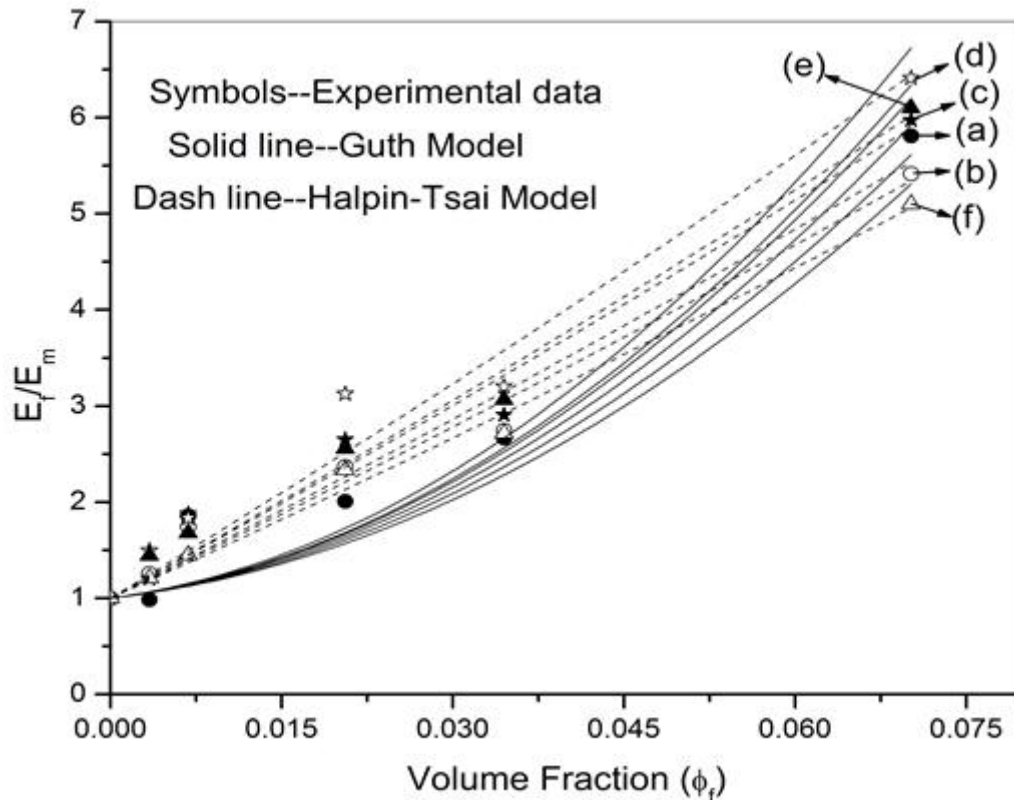


Fig. 7. Halpin-Tsai and Guth model fittings for nanocomposites irradiated at different doses (a) 50 kGy (b) 100 kGy (c) 150 kGy (d) 200 kGy (e) 250 kGy (f) 300 kGy

#### 4. Conclusion

The study confirmed that high energy radiation substantially improves the physico-mechanical properties polymer blends, and the morphology of the blends can affect the radiation processing of polymer blends based nanocomposites. SBR/ EPDM system was found to be immiscible in nature. Gel fraction of the blends increased with the increase in EPDM content in the blend but not in the proportion predicted by weighted average calculations. Tensile strength, hardness studies showed a good agreement with gel content studies. Reduction in elongation at break of the blends with increase in radiation dose was attributed to prevention of the structural organization during drawing due to the formation of crosslinked network. These studies also showed that the irradiation of SBR/PDM blends to a threshold dose induces good compatibility between the two components SBR and EPDM which otherwise show poor compatibility. Addition of MWNT resulted in enhanced radiation sensitivity of SBR/EPDM/MWNT nanocomposites that was attributed to the enhanced probability of spur overlap, due to the reduction in the free volume of the nanocomposite matrix with higher MWNT content. This led to higher tensile strength, hardness and density. Elastic modulus increased with the radiation dose while elongation at break decreased with dose. The Halpin-Tsai model fitted better into the experimentally observed modulus values and predicted low aspect ratio of MWNT in the matrix, indicating agglomeration of MWNTs.

#### References

1. R. L. CLOUGH, Nuclear Instruments And Methods In Physics Research, Section B: Beam Interactions With Materials And Atoms, 185 (2001). P. 8.
2. Z. P. ZAGÓRSKI, Radiation Physics And Chemistry, 71 (2004). P. 261.
3. J. SHARIF, S. H. S. A. AZIZ, AND K. HASHIM, Radiation Physics And Chemistry, 58 (2000). P. 191.
4. V. PLAČEK, B. BARTONÍČEK, V. HNÁT, AND B. OTÁHAL, Nuclear Instruments And Methods In Physics Research, Section B: Beam Interactions With Materials And Atoms, 208 (2003). P. 448.
5. S. CHEN, J. ZHANG, AND J. SU, Journal Of Applied Polymer Science, 114 (2009). P. 3110.
6. F. CIARDELLI, S. COIAI, E. PASSAGLIA, A. PUCCI, AND G. RUGGERI, Polymer International, 57 (2008). P. 805.
7. J. SHARIF, K. Z. M. DAHLAN, AND W. M. Z. W. YUNUS, Radiation Physics And Chemistry, 76 (2007). P. 1698.
8. E. T. B. MCDONEL, K. C.; ANDRIES, J. C. , Elastomer Blends In Tyres. , In Polymer Blends, D.R.A.N. Paul, S., Editor. 1978, Academic Press: New York. P. 287.
9. S. C. GEORGE, K. N. NINAN, G. GROENINCKX, AND S. THOMAS, Journal Of Applied Polymer Science, 78 (2000). P. 1280.
10. C. V. CHAUDHARI, Y. K. BHARDWAJ, N. D. PATIL, K. A. DUBEY, V. KUMAR, AND S. SABHARWAL, Radiation Physics And Chemistry, 72 (2005). P. 613.
11. S. H. EL-SABBAGH, Polymer Testing, 22 (2003). P. 93.
12. A. A. BASFAR AND J. SILVERMAN, Radiation Physics And Chemistry, 46 (1995). P. 941.
13. J. SHARIF, W. M. Z. W. YUNUS, K. Z. H. M. DAHLAN, AND M. H. AHMAD, Polymer Testing, 24 (2005). P. 211.
14. P. THAVAMANI AND D. KHASTGIR, Journal Of Elastomers And Plastics, 29 (1997). P. 124.
15. A. CHARLESBY, Radiation Physics And Chemistry, 9 (1977). P. 17.
16. B.-S. CHIOU, S. R. RAGHAVAN, AND S. A. KHAN, Macromolecules, 34 (2001). P. 4526.
17. J. C. HALPIN AND J. L. KARDOS, Polymer Engineering And Science, 16 (1976). P. 344.
18. D. ALMECIJA, D. BLOND, J. E. SADER, J. N. COLEMAN, AND J. J. BOLAND, Carbon, 47 (2009). P. 2253.

19. F. M. BLIGHE, P. E. LYONS, S. DE, W. J. BLAU, AND J. N. COLEMAN, Carbon, 46 (2008). P. 41.